

Changes in the State of the Material by Shot Peening

O. Vöhringer, Institut für Werkstoffkunde I, Universität Karlsruhe (TH), FRG

1. Introduction

Shot peening is a frequently used mechanical treatment to modify the surface state of a material. It is applied for the purpose of improving the fatigue strength and the fatigue life, respectively, when subjected to cyclic loading as well as the corrosion fatigue behaviour, the stress corrosion cracking, the fretting corrosion and the wear resistance (cf. 1, 2). It is also well known that shot peening lowers the proof and the buckling stresses (3) combined with alterations in the workhardening behaviour (cf. 3, 4). Thus, to evaluate the consequences of shot peening on the behaviour of mechanically loaded parts, all changes of the surface state have to be determined exactly. In the following review, after discussing some details concerning the formation processes of a peened surface condition, the most important methods and properties to describe this material state are presented. Then, the effects of the different peening parameters on the surface state will be regarded and characteristic examples of the peening-induced changes of the surface state will be presented and discussed. Finally, the stability of the peened condition, especially of the residual stress state during thermal or mechanical loading, is briefly examined.

2. Development of the surface state during shot peening

Shot peening of metallic materials causes inhomogeneous plastic deformations of the near surface layers. The most important deformation processes occurring are schematically given in Fig. 1.

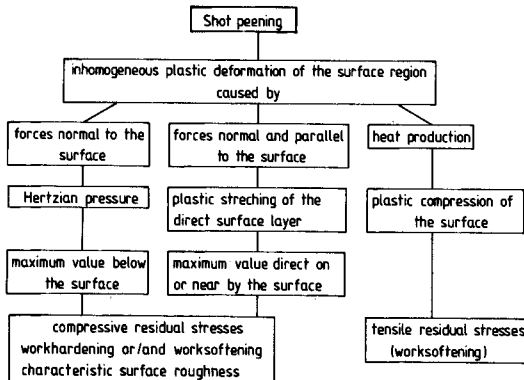


Fig. 1: Shot peening processes and work-piece reactions (8)

These processes are, on the one hand, the Hertzian pressure with maximum values of the forces below the surface and, on the other hand, the plastic stretching of the near surface layer with maximum forces at the surface itself (6 - 8). Thereby compressive residual stresses with characteristic depth distributions are produced together with workhardening and/or worksoftening effects and typical surface topographies are created. The maximum of the compressive residual stresses may be situated below the surface (especially for hard materials) or directly at the surface (especially for soft materials) according to the dominating process. In all materials, a peening-induced adiabatic heat production is expected accompanied with a rise in temperature. This effect is caused by extremely short impact durations of the concerning shot together with plastic deformation of various degrees according to the hardness of the material (9). In soft materials, it is possible that a sufficient rise in temperature may produce plastic compression of the surface together with a reduction of the shot peening residual stresses.

The above described processes are influenced by a complex interaction of a variety of parameters summarized in Tab. 1. These are divided into two groups which are characterized by either the shot peening or the workpiece conditions. The two parameter groups, however, are largely interactive. The shot peening parameters may have typical influences on the workpiece properties (e. g. sections 4 and 5).

Shot peening parameters	
<u>shot peening conditions</u>	<u>workpiece conditions</u>
<ul style="list-style-type: none"> • type and density • shape, diameter and size distribution • hardness • velocity or pressure • exposure time or coverage • impact angle • mass flow • nozzle diameter • distance from nozzle to workpiece 	<ul style="list-style-type: none"> • hardness or yield point • workhardening rate • residual stresses • surface topography • phase composition • phase stability • defects in the surface layer

Table 1: Shot peening parameters

Several models were developed to analytically describe the surface state, especially the distributions of strains, stresses and residual stresses during and after the peening process, respectively (5, 9 - 13). The models result essentially from considerations not only of the quasistatic penetration but also of the dynamic impact of a single ball in the workpiece (6, 9 - 11). Moreover, the workpiece reactions which are caused by shot peening are discussed taking into consideration repeated deformations including the Bauschinger-effect and the cyclic deformation behav-

four of the material (12, 13). In most cases, modelling of the residual stresses proves that the distributions are only qualitatively in agreement with experimental results. Therefore, the details of these theoretical considerations must be considerably improved. Especially the postulated boundary conditions and processes or material laws should be reflected on and modified.

3. Properties of the peened surface region

To describe the condition of a shot peened surface sufficiently, it is necessary to know the characteristics of the different testing methods. The testing methods and properties which have been applied up to now are summarized in Tab. 2. The best known

Table 2: Methods and properties to characterize the shot peened surface state

Methods and properties to characterize the shot peened surface state
<ul style="list-style-type: none"> • microhardness HV • residual stress σ^{rs} • half width value HW • root-mean-squared strain $\langle \epsilon^2 \rangle^{1/2}$ and particle size L • dislocation density $\rho_T = \frac{2\sqrt{3}}{b} \cdot \frac{\langle \epsilon^2 \rangle^{1/2}}{L}$ • Almen intensity $i-v \cdot d \cdot t$ • texture pole figures and lattice deformation pole figures • surface roughness R_f • plastic strain ϵ_p • phase fraction (e.g. retained austenite) f • fraction of deformation twins f_T • transmission electron microscopy • surface yield point R_0^s • temperature T

properties are the micro-hardness HV, the residual stresses σ^{rs} (usually determined by X-ray diffraction or mechanical methods) and the half-width values HW of the X-ray interference lines. The HW-values characterize the occurring lattice distortions and micro-residual stresses, respectively. An example of the depth distributions of the properties HV, HW and σ^{rs} obtained by X-ray diffraction and successive electrolytical surface removal is given in Fig. 2 for the shot peened titanium-alloy TiAl6V4 (14). Maximum compressive residual stress amounts (830 N/mm^2) occur at a depth of 0.1 mm. The penetration depth of the peening process is evaluated from the σ^{rs} - and HW-distributions and amounts to approximately 0.4 mm. As can be seen, the half-width values show a much more sensitive reaction compared to the micro-hardness, if changes in the material state caused by shot peening occur. This finding is generally valid and plausible taking into consideration that the micro-hardness penetration itself produces a relative severe interference in the materials state.

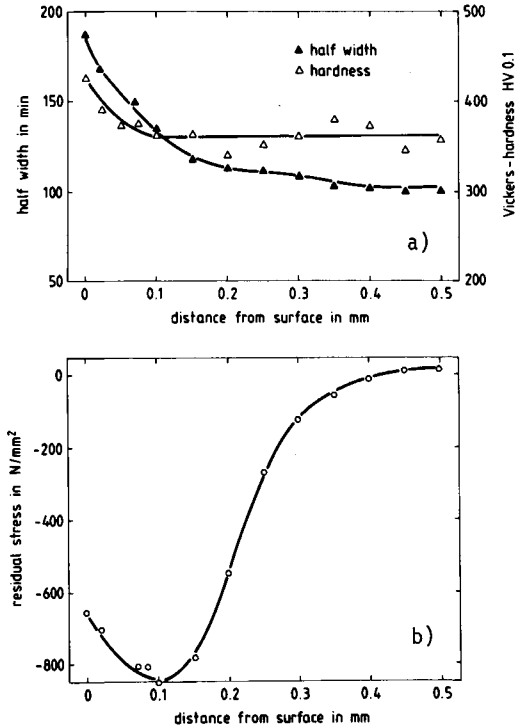


Fig. 2: Distributions of a) half-width values and Vickers-hardness HV0.1 and b) residual stresses of shot peened TiAl6V4 in an as received condition (S 170, $p = 1,6$ bar, coverage 300 %) (14)

X-ray stress measurements, which offer the possibility of integrating over large surface areas of a plane surface, in most cases lead to standard deviations of the residual stresses of only a few N/mm^2 . However, measurements of a shot peened surface with a very thin screened X-ray beam reveal considerable differences in the residual stresses of different surface points. Fig. 3 gives the appropriate residual stresses and half-width values for the plain carbon steel Ck 45 in the normalized and shot peened condition (15). For these measurements, a circular aperture with 0,23 mm diameter only was used. Several σ^{rs} -values determined at distinct points over a linear distance of 2.5 mm with a measuring time of 5 hours per value are given in Fig. 3. The σ^{rs} -values fluctuate between -180 N/mm^2 and -500 N/mm^2 with considerable standard deviations of about $\pm 50 \text{ N/mm}^2$. These findings are understandable taking into consideration the fact that the impression area of one ball has nearly the same size as the X-ray spot. The measured residual stress differences shown in Fig. 3 are nearly as large as those measured at shot impressions produced with significantly larger balls (16). Further residual stress measurements of the same surface region of the shot peened Ck 45 with a slit aperture of $6 \times 0,5 \text{ mm}^2$ lead to $\sigma^{rs} = -369 \pm 4 \text{ N/mm}^2$. This value is in good agreement with the mean value (dashed curve) in Fig. 3. As can be seen, the standard deviations are one order of magnitude smaller than in the case of the thin screened X-ray beam. In the lower part of Fig. 3, the half-width

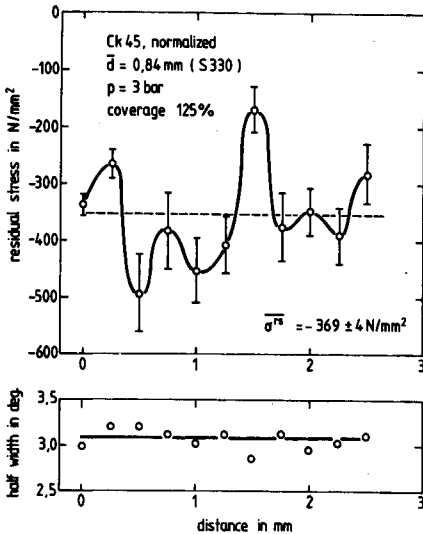


Fig. 3: Residual stresses and half-width values of the shot peened plain carbon steel Ck 45 (0.45 wt.-% C) in the normalized state determined at distinct points with a circular aperture of 0.23 mm diameter (15)

values show only relatively small fluctuations which do not coincide with the appertaining σ^{RS} -changes. This means that in spite of considerable local residual stress variations after peening, a homogeneous workhardening state exists in a good approximation in the direct surface layer. Thus, in the discussion and in the modelling of the consequences of shot peening residual stresses on loaded components, the existence of these σ^{RS} -fluctuations should be taken into account.

From the profile analyses of the X-ray interference lines according to Warren-Averbach (cf. 17, 18) one obtains extended and improved results concerning the surface state. The mean distortions $\langle \epsilon^2 \rangle^{1/2}$ determined with this method are directly proportional to the micro-residual stresses. The $\langle \epsilon^2 \rangle^{1/2}$ -values may be caused by the intrinsic stress fields of dislocations and of soluted alloying atoms. The particle size L indicates the size of coherent scattering regions. L is related with dislocation spaces and cell sizes in deformed or hardened materials (17, 18). With regard to distinct boundary conditions, the total dislocation density can be calculated from the properties $\langle \epsilon^2 \rangle^{1/2}$ and L using the relationship

$$\rho_t = \frac{2\sqrt{3}}{b} \cdot \frac{\langle \epsilon^2 \rangle^{1/2}}{L} \quad (1)$$

(b = amount of the burgers vector of a dislocation). The ρ_t -values are in good agreement with those estimated with TEM investigations (19).

A technological measure of the changes of the surface state is the well-known Almen-intensity, which is defined by the deflection resulting from the shot peening of a plate of normed size, the so-called Almen strip. The empirically determined shot intensity is approximately proportional to the product of shot velocity v , shot size d and shot time t ($i \sim vdt$).

As during shot peening inhomogeneous plastic deformations occur in the surface layer rapidly decreasing to zero in a depth of a few tenths of a millimeter, typical textures will be generated. The knowledge of these textures is also necessary to allow a complete description of the surface state. The shot peening textures can be illustrated in so-called texture pole figures as shown exemplarily in Fig. 4 for a quenched and tempered Ck 45 in two different representations. The left hand pole figure includes in a plane description 10 intensity contour lines, where I_{\min} has the level "zero" and I_{\max} the level "10". In the right hand figure, the intensity data are represented three-dimensionally. In this case, a rotation symmetrical $\{211\}\langle uvw \rangle$ -fibre texture occurs (20). In textured surfaces, additional information concerning the two-dimensional residual stress state can be obtained with the aid of lattice strain pole figures (21, 22).

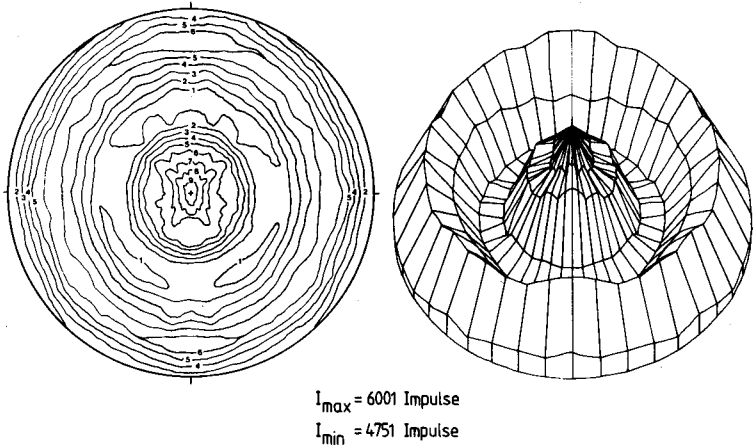


Fig. 4: $\{211\}$ -texture pole figure of shot peened Ck 45 in a quenched and tempered state (S 230, $v = 53 \text{ m/s}$, coverage 300 %) (20)

It should be further mentioned that the surface topography and the distribution of plastic strains are also important properties of the peened surface. The latter can be estimated for example from single ball tests applying a measuring grid (5, 9). In a normalized Ck 45, surface plastic strain values in the order of magnitude of 10 % were evaluated with this method. Similar strain values are reported by (23) comparing the half-width values of shot peened steels with those of corresponding specimens deformed in compression tests with usual strain rates. Transmission electron microscope investigations at normalized 35Cr4 with an exact target preparation show dislocation structures with cells and tangles (23) as can usually be observed at uniaxial deformation, but not at cyclic deformation. The dislocation densities decrease with increasing distance from the surface in a manner similar to the half-width values of the X-ray interference lines.

Additional information regarding the peened surface state, can be obtained for specific materials by analyzing the microstructure. This method is useful if materials with metastable phases are shot peened because transformation induced plasticity can occur, as for example the transformation of retained austenite in martensite in hardened steels (24 - 26). Furthermore, conclusions regarding the deformation and stress state can be drawn from the existence and the frequency of deformation twins which are produced in the surface region of peened materials having a sufficiently small stacking fault energy.

It should also be mentioned that sensitive thermometric investigations of the temperature changes (27) allow to make indirect statements of the peening induced deformation states. Finally, another method should be mentioned with which the yield point $R_{0.2}$ of a peened surface layer can be determined (28, 29). This yield point can be analyzed using combined mechanical and X-ray measurements with discrete increases of compression loading and unloading up to the critical loading stress, where the relaxation of residual stresses starts. With this method, peening induced workhardening and worksoftening effects, respectively, could be observed in different materials (28, 29).

4. Effects of Different Parameters

All shot peening parameters listed in Tab. 1 can change the materials state in many ways. This is already reviewed in several investigations (e. g. 1, 2, 6, 7, 26, 30), and therefore, only the most important aspects will be mentioned here. With regard to the development of shot peening residual stresses, the workpiece hardness has proved to be a very useful order parameter (7, 29).

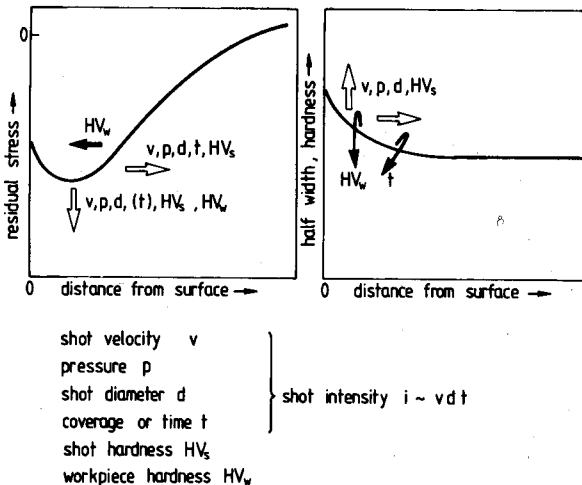


Fig. 5: Influence of different properties on the residual stress distributions, the half-width values and the hardness, resp. (33)

Fig. 5 shows schematically and in a rather simplified way the observed influences of the shot intensity i , the shot hardness and the workpiece hardness on the depth distribution of the residual stresses as well as the hardness and the half width. As can be seen, the curves are shifted in the direction of the arrows with increasing parameters. For example, the increasing of nearly all parameters results in an increase in the maximum of the compressive residual stresses. With the exception of the workpiece hardness, the penetration depth of the shot peening induced residual stresses also increases. This effect often produces a workhardening of the surface layer indicated by increasing half-width values. However, in relatively hard materials, such as hardened steels or cold formed materials, the peening process causes worksoftening effects. Finally, it can generally be stated that with increasing shot time and multiple coverage, respectively, a worksoftening effect also occurs which is initiated by fatigue processes as e. g. cyclic deformation, crack formation and crack propagation (31, 32).

Only a few systematic investigations exist which examine the influence of the shot peening angle on the surface condition (cf. 33, 34). In the following, some recent results obtained at normalized plain carbon steels Ck 45 shall be presented (33). Fig. 6 shows the shot peening residual stress distributions in longitudinal ($\phi = 0^\circ$) and transverse ($\phi = 90^\circ$) directions and the respective shot peening angles in the range $90^\circ < \alpha < 45^\circ$. The residual stress values were obtained by the X-ray diffraction method. In longitudinal direction ($\phi = 0^\circ$), the surface compressive residual stresses as well as the maximum compressive residual stress values, which lie in a depth of about $50 \mu\text{m}$, and also the penetration depth decrease with decreasing peening angle α . This can be attributed to a decreasing effect of the peening intensity. However, in transverse direction ($\phi = 90^\circ$) an anomalous behaviour can be observed. The maximum compressive residual stresses below the surface increase with decreasing angle α . This phenomenon is caused by a more pronounced workhardening effect

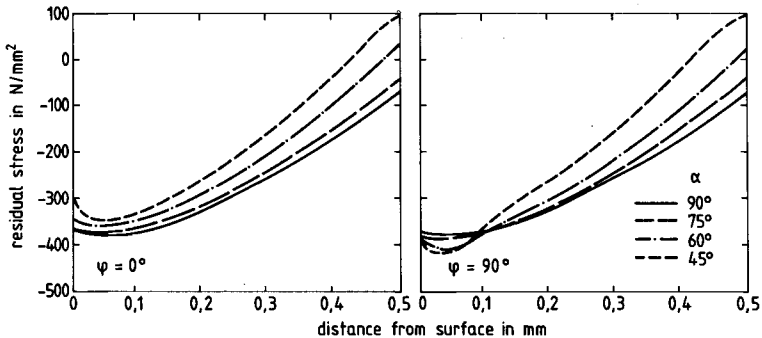


Fig. 6: Residual stresses of normalized Ck 45 shot peened at different impact angles vs. distance from the surface ($S\ 330$, $p = 3\ \text{bar}$, coverage 100 %) (33)

occurring in transverse direction (33). The appertaining $\{110\}$ -texture pole figures for the peening angles $\alpha = 90^\circ$ (left-hand side) and 45° (right-hand side) are presented in Fig. 7. During perpendicular shot peening ($\alpha = 90^\circ$), a rotation symmetrical $\{110\}$ -fibre texture is generated. This means that the slip planes of the bcc-ferrite lattice will mainly be straightened parallel to the surface and will thus facilitate the occurrence of plastic stretching effects in the surface region. Inclined shot peening ($\alpha = 45^\circ$) produces a texture which is analogous to that appearing after perpendicular peening. The poles, however, are tilted by an angle of 16° (see Fig. 7b).

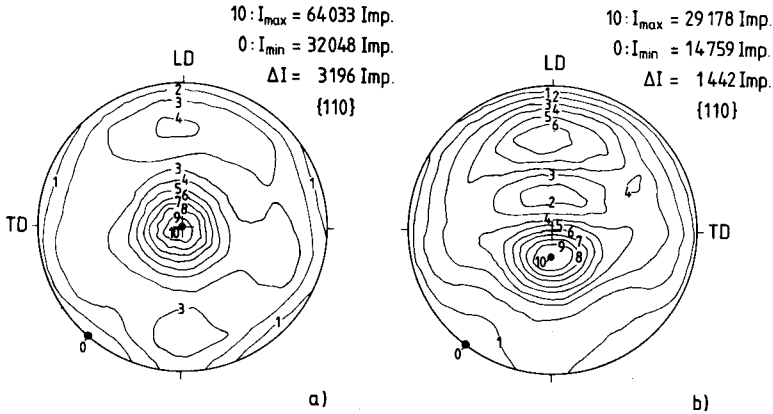


Fig. 7: $\{110\}$ -texture pole figures of normalized Ck 45 shot peened a) perpendicular to the surface ($\alpha = 90^\circ$) and b) inclined to the surface ($\alpha = 45^\circ$) (LD = longitudinal direction = shot peening direction, TD = transverse direction; S 330, p = 3 bar, coverage 100 %)

5. Characteristic examples of the influence of the workpiece state

The influence of different workpiece states before peening on the shot peened surface state shall be discussed in the following section by the aid of selected examples. In this connection, the workpiece hardness is the most important property (6). As can be seen from several examples in Fig. 8, the amounts of the surface compressive residual stresses σ_s^{RS} and of the maximum compressive residual stresses beneath the surface σ_{\max}^{RS} at first increase fast and then slower with increasing hardness. σ_s^{RS} even approaches a limiting value. In soft materials, there are no or relatively small differences between both properties, which is a consequence of the dominating stretching effects occurring during shot peening. In this case, the surface workhardening results in an increase in the amount of the residual stresses which even can ex-

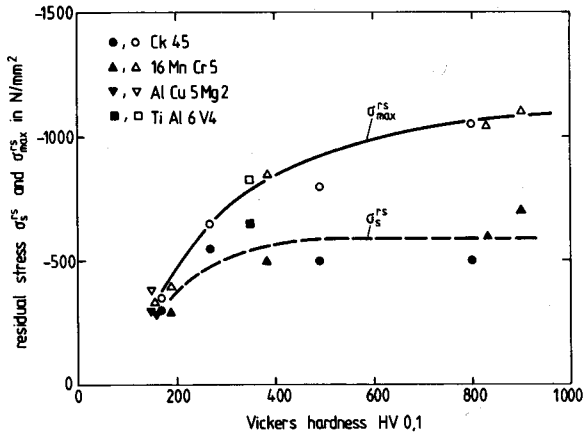


Fig. 8: Surface residual stresses σ_s^{rs} and maximum residual stresses σ_{max}^{rs} of shot peened materials vs. Vickers hardness HV 0.1 (from 14, 28, 35 - 38)

ceed the yield point of the unpeened condition. However, with increasing hardness, the difference between surface and maximum residual stresses also increases. This effect can be attributed to the Hertzian pressure which dominates more and more. In the upper part of Fig. 9, this effect is again illustrated by the residual stress distributions of a shot peened Ck 45 in the normalized, quenched and tempered and quenched condition (8). Although the individual results are not fully identical with regard to the shot peening parameters used (they are taken from (20, 35)), they confirm the above stated facts. The lower part of Fig. 9 shows the appertaining depth distributions of the changes in the hardness $\Delta HV 0.1$ and the half-width values ΔHW . It is quite obvious that the normalized condition shows in the peening-induced surface region $\Delta H 0.1$ - and ΔHW -values which have the same sign. In contrast, this is not the case in the quenched and tempered and in the quenched condition. In the second case, the peening process causes an increase in the surface hardness and a decrease in the appertaining half-width values. With increasing distance from surface, $\Delta HV 0.1$ passes through a maximum and then falls to zero. At the maximum of $\Delta HV 0.1$, the half-width holds minimum values. ΔHW -values can be measured down to a depth of 0.4 mm. In the quenched and tempered condition, the half-width values not only increase in the near surface region, but also decrease in greater depths.

The fact that shot peening results in different changes of micro-hardness and half-width values can - with regard to the work-hardening and worksoftening effects at the surface - mainly be attributed to the influence of compressive macro-residual stresses on the hardness measuring procedure (31, 35). Thereby, the existing hydrostatic compressive residual stress state puts up an additional resistance to the indenter during the hardness test

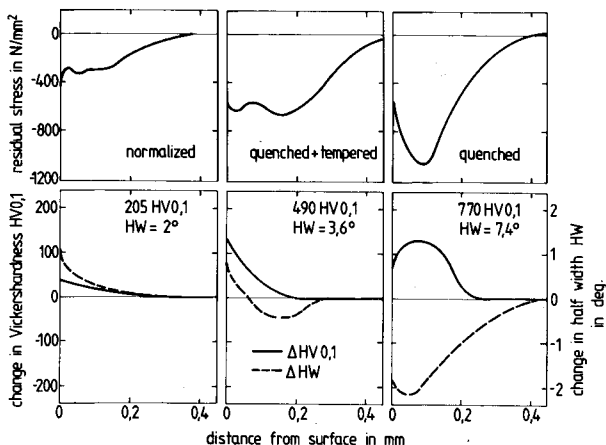


Fig. 9: Residual stresses and changes in Vickers-hardness HV0.1 and half-width values, resp., of shot peened Ck 45 in normalized, quenched and tempered, and quenched conditions (8)

and thus leads to smaller hardness impressions. This means that higher hardness values are achieved in comparison with a residual stress-free material which has the same half-width values at the surface. Experiments carried out by (35, 36) allow the estimation of a linear hardness increase of about 12HV0.1 at an increase of the amount of the compressive residual stresses of 100 N/mm². Consequently, the determined hardness increase in the near surface region of shot peened materials is only fictitious and not compatible with the behaviour of the half-width values.

Frequently, a decrease of the half-width values during peening of quenched and in some cases of quenched and tempered steels was observed (cf. 1, 2, 8, 20, 35 - 38). This phenomenon is in fact attributed to worksoftening effects as shown by the Warren-Averbach profile analysis at plain carbon and low alloyed steels after different heat treatments (17). A typical result is presented in Fig. 10. Fig. 10a shows as a measure of the micro-residual stresses the mean distortions $\langle \epsilon^2 \rangle^{1/2}$ versus the hardness of the unpeened steels. In the unpeened condition, these values increase considerably with increasing hardness. This effect is caused by the increasing dislocation density and an increasing content of carbon atoms in solid solution (18). At lower hardness values (< 500HB and 50HRC, resp.) increasing $\langle \epsilon^2 \rangle^{1/2}$ -values are observed during the peening process. This workhardening process is the more effective the smaller the hardness values are. However, peening of steels with hardness values > 500HB (and > 50HRC, resp.) results in decreasing $\langle \epsilon \rangle^{1/2}$ -values in a manner analogous to the decreasing half-width values. The appropriate worksoftening effect is the more effective the more the hardness increases. Furthermore, Fig. 10b shows that the particle size values are reduced by peening. This effect is strengthened the smaller the

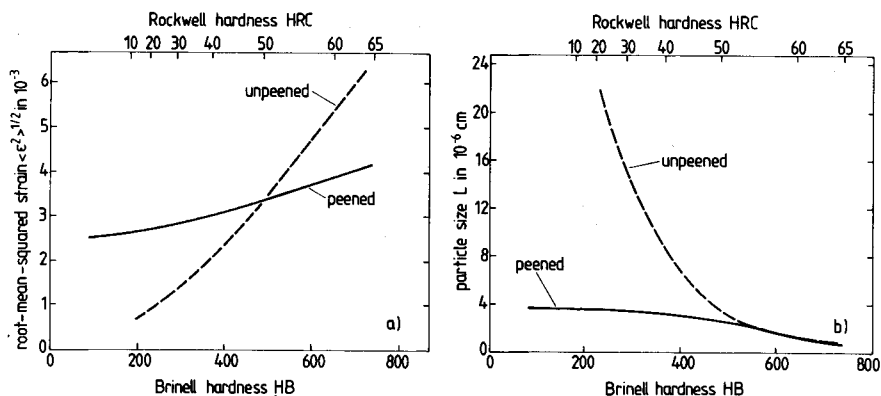


Fig. 10: Effects of hardening and shot peening on a) root-mean-squared strain $\langle \epsilon^2 \rangle^{1/2}$ and b) particle size L for several plain carbon and low alloyed steels (17)

workpiece hardness is. For hardness values $< 500\text{HB}$, the estimation of the dislocation densities ρ_t in the direct surface with eq. (1) yields ρ_t -values which are higher in peened surfaces than in unpeened surfaces. This means that in this case the workhardening effect is only caused by the dislocation hardening mechanism. However, the reduction of the mean distortion values $\langle \epsilon^2 \rangle^{1/2}$ can only be observed in the martensitic state and in the quenched and tempered state (hardness $> 500\text{HB}$), which are characterized by relatively high dislocations densities (39). The decrease of $\langle \epsilon^2 \rangle^{1/2}$ is partly caused by a rearrangement of dislocations into arrangements of lower distortion energy. Furthermore, in connection with the movement of the slip dislocations, the soluted carbon atoms move from their original octahedral sites to other octahedral sites, which are favoured by the dislocation stress fields by the so-called Snoek-effect. Thereby, the tetragonal distortion of the martensite lattice by soluted atoms, influencing the $\langle \epsilon^2 \rangle^{1/2}$ -values, will be reduced (40). Moreover, it cannot be excluded that peening induced increases in the temperature and subsequent annealing effects lead to an additional decrease of the $\langle \epsilon^2 \rangle^{1/2}$ -values.

Compared to the peening behaviour of hardened steels, there is only little knowledge of the fact that cold-formed materials also show peening induced worksoftening effects (41, 42). An example of this is presented in Fig. 11 which shows measurements of the micro-hardness HV 0.3 in dependence of the distance from surface of a shot peened Ck 45. After being normalized, this steel was cold-rolled and shot peened. With increasing rolling deformation, a more pronounced worksoftening effect occurs which exists down to a depth of about 0.4 mm. This effect is obviously caused by the rearrangement of the rolling dislocation structure in a more favourable shot peening dislocation structure. Unfortunately, corresponding TEM-investigations are missing.

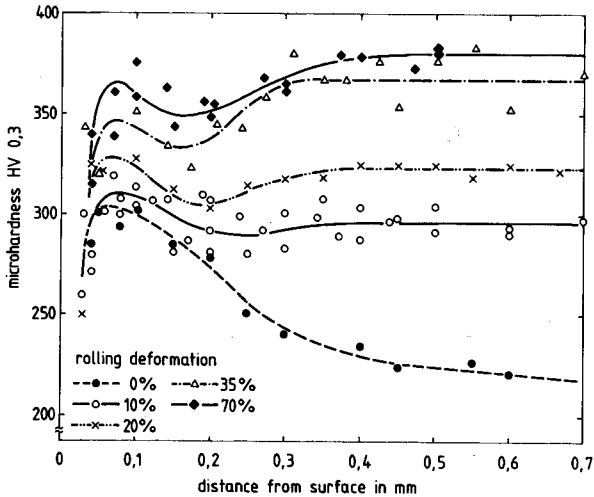


Fig. 11: Micro-hardness HV0.3 of Ck 45 after rolling and shot peening vs. distance from surface (S 330, p = 3, coverage 100 %) (42)

All mentioned worksoftening effects, which are induced by the shot peening process in hardened steels or cold-formed materials with a coverage of 100 %, can occur without the appearance of fatigue processes, i. e. of low cycle fatigue and crack initiation. Of course, these mechanisms gain growing significance with increasing shot peening time and coverages greater than 100 %.

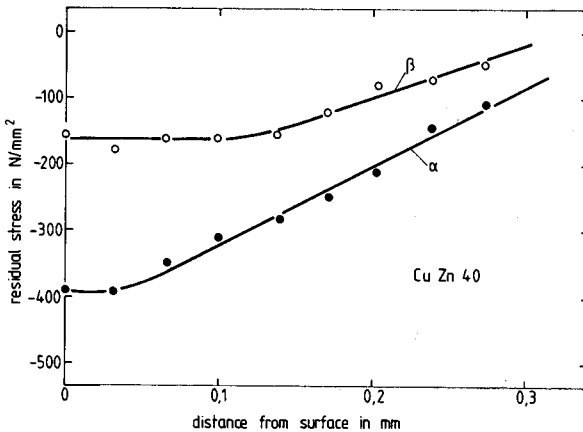


Fig. 12: Residual stresses in the α -phase and the β -phase of a shot peened CuZn40 vs. distance from surface (S 170, p = 0,24 bar, coverage 100 %) (20)

An interesting and fundamental problem arises when coarse multiphase materials are shot peened and the phases reveal different deformation and workhardening effects during the generation of residual stresses (43, 44). For example in Fig. 12, the depth distributions of the residual stresses after peening of the (α + β)-copper-zinc alloy CuZn40 of both phases (75 Vol.-% fcc. α -phase and 25 Vol. % bcc. β -phase) are shown. In each case, the residual stress distributions result from the superposition of the residual macro- and micro-stresses. Since the β -phase shows a stronger workhardening effect and thus a smaller compression deformation of the β -grains, the produced amounts of the mean residual stresses are smaller than in the α -phase. With the aid of a mixture rule (43), the residual micro-stresses in the direct surface can be estimated to $+180 \text{ N/mm}^2$ in the β -phase and -60 N/mm^2 in the α -phase with a mean residual macro-stress of -330 N/mm^2 .

As a further example of the surface state of multiphase materials, Fig. 13 shows the hardened tool steel X210Cr12 (2,1 wt.-% C, 12 wt.-% Cr) which includes the phases martensite, retained austenite and chromium carbide Cr_7C_3 . The typical distributions of the shot peening induced residual stresses and the half-width values in the martensite phase (see Figs. 13a and b) can be seen as well as the depth distributions of the retained austenite at different austenitisation temperatures (Fig. 13c). The residual

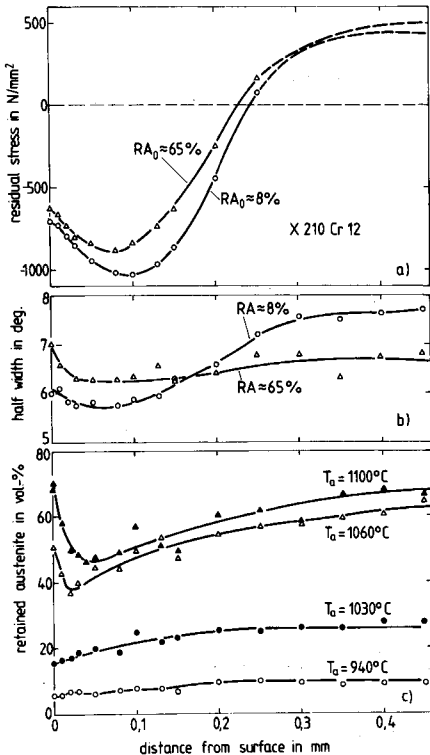


Fig. 13: Residual stresses, half-width values and retained austenite of shot peened X210Cr12 in a quenched state vs. distance from surface (S 330, $p = 3 \text{ bar}$, coverage 100 %) (42)

stress amounts in the martensite phase decrease with increasing contents of retained austenite. With the exception of the direct surface region ($< 40 \mu\text{m}$), the half-width values in the peening induced region are smaller than in larger depths. In this case, the martensite also shows a worksoftening effect which is more pronounced at a smaller content of retained austenite. As can be seen from the HW-distribution in the direct surface layer of a thickness of $40 \mu\text{m}$ a workhardening effect is superimposed on the general worksoftening behaviour. A distinct transformation induced plasticity effect (TRIP-effect) of retained austenite in martensite will be produced by the peening process as shown for instance in Fig. 13c. In the direct surface layer ($< 40 \mu\text{m}$) of this steel, however, a reduced TRIP-effect occurs at high contents of retained austenite (65 % and 80 % in the unpeened condition). In this relatively soft layer, it may be possible that a peening induced temperature increase - combined with a thermo-mechanical stabilization of the retained austenite - lowers the martensite start temperature and therefore increases the content of the retained austenite.

TRIP-effects occurring during shot peening can also be observed at manganese steels with relatively high manganese contents (45). In Fig. 14, the corresponding hardness distributions obtained after shot peening of three steels with different manganese contents are plotted. The metastable steels X115Mn4 and X115Mn6 show shot peening induced TRIP-effects, which means that martensite will be produced in the near surface region (45). As is illustrated in Fig. 14, this martensite produces appropriate hardness increases. The so-called Hatfield steel X115Mn12 indicates no martensite formation. The workhardening effect in this steel rather results from dislocation hardening and an extensive mechanical twin deformation combined with dynamic strain aging effects (45).

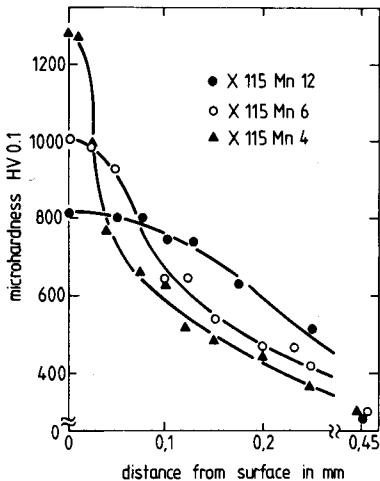


Fig. 14: Micro-hardness HV0.1 of different shot peened manganese steels vs. distance from surface (S 230, $p = 10 \text{ bar}$, $t = 5 \text{ min}$) (45)

The improvement of the properties of components with defectively treated surfaces (cf. during grinding or heat treatment etc.) by additional shot peening is of high interest for practical applications. In this respect, it can generally be stated that the "defective prehistory" can largely be eliminated by shot peening if the peening process affects deeper areas than the observed defects. The following figures supply some useful information concerning this phenomenon. Fig. 15 presents distributions of residual stresses and half-width values of ground and subsequently peened specimens of hardened Ck 45 (36). The ground materials state, which is characterized in Fig. 15 by compressive residual stresses and reduced half-width values in the direct surface layer of 20 μm thickness, is completely changed by shot peening. Accordingly, typical σ^{RS} - and HW-distributions exist as was already discussed above. The behaviour of shot peened case-hardened

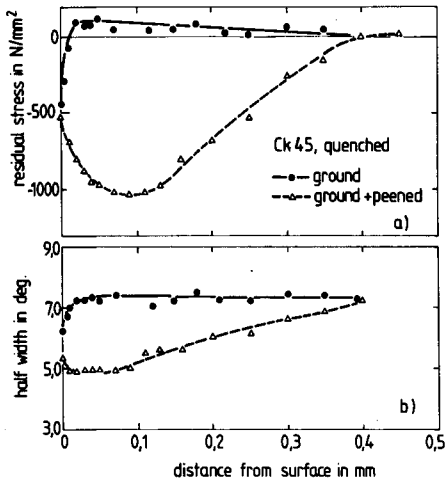


Fig. 15: Residual stresses and half-width values of quenched and ground Ck 45 in an unpeened and a shot peened state vs. distance from surface (S 230, $p = 4,7$ bar, coverage 400 %) (36)

steels is similar (see Fig. 16). The carbon gradient is an important influencing factor on the formation of the σ^{RS} - and HW-distributions before and after peening (37, 38). The compressive residual stresses occurring after shot peening are similar to those of hardened steels with homogeneous carbon distributions. With the exception of a surface layer of 10 μm thickness, the HW-values are smaller after peening compared to the unpeened state. This observation is attributed to worksoftening effects which are analogous to the results shown in Figs. 9 and 10. In this case, surface oxidation effects which may occur sometimes during the case hardening process do not influence the σ^{RS} - and HW-distributions existing after peening (37, 38).

Finally, the surface state of the decarburized and quenched and tempered spring steel 55Cr3 in the unpeened and the shot peened condition is illustrated in Fig. 17 by means of the residual stress distributions and the half-width values (46). The tensile residual stresses, which are caused by decarburization of the surface region having a maximum of nearly 350 N/mm² in a depth of

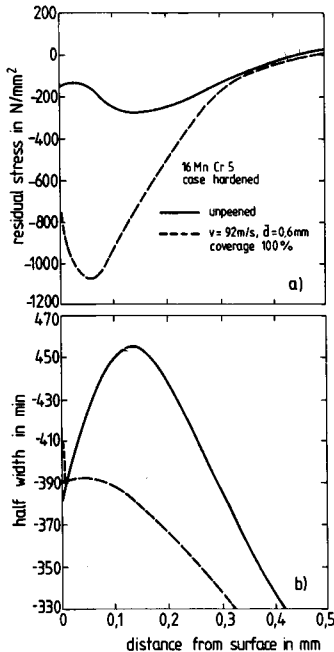


Fig. 16: Residual stresses and half-width values of case hardened 16MnCr5 in an unpeened and a shot peened state vs. distance from surface ($d = 0.6$ mm, $v = 92$ m/s, coverage 100 %) (37, 38)

100 μm , are completely rearranged by peening. As can be seen from the HW-distribution, a workhardening effect is observed in the direct surface layer (< 40 μm) and a worksoftening effect in the interior region (between 40 μm and 350 μm). Variations of the surface decarburizing effect and possible surface oxidation have only a very small influence on the peening induced σ^{RS} - and HW-distributions (46). This means that variations of the defects result in no or only slight changes of the mechanical properties of the peened components.

6. Stability of the peened surface state

The stability of the peened surface state in components during the application of thermal and/or mechanical energy is desirable in order to preserve the improvements in the mechanical properties. In this connection, the residual stress behaviour is the most important aspect to be considered. Macro- and micro-residual stresses can be reduced or completely relaxed either by heat treatment or under unidirectional or cyclic mechanical loading as reported in detail by (4, 47, 48).

Elastic residual strains related to residual stresses can be converted into microplastic strains by suitable deformation processes, as for example by dislocation slip or creep. The onset of residual stress-relaxation depends on the resistance R_i to the onset of plastic deformation. In the case of unidirectional deformation, R_i is given by the yield point R_e or the proof stress $R_{p0.01}$. Accordingly, at cyclic loading, $R_i = R_{e,cyc}$ (cyclic yield

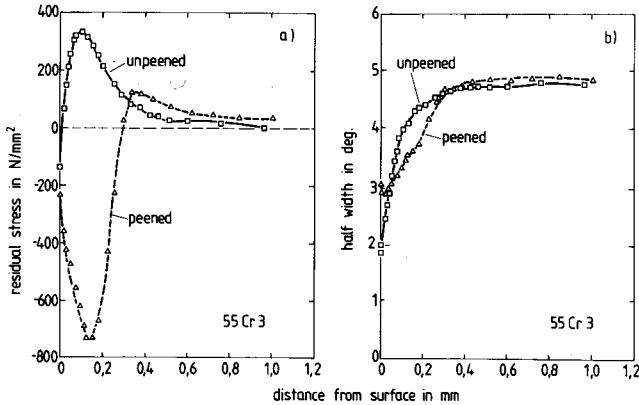


Fig. 17: Residual stresses and half-width values of decarburized, quenched and tempered spring steel 55Cr3 in an unpeened and a shot peened state vs. distance from surface ($d = 0,8 \text{ mm}$, Almen intensity $A_2 = 0.52 \text{ mm}$) (46)

point) is valid, and at heat treatment $R = R_{e,c}$ (creep resistance limit) is valid. In principle, residual stress-relaxation occurs when the linear superposition of a predominantly uniaxial state exists according to

$$\sigma + \sigma^{rs} = R_i \quad (2).$$

Residual stress-relaxation does not occur if the condition

$$\sigma + \sigma^{rs} < R_i \quad (3)$$

is fulfilled (4, 48).

The applied stress σ may be zero, have a value which does not vary with time (cf. thermal residual stress-relaxation), have a steadily increasing value (cf. unidirectional deformation) or a value varying periodically with time (cf. cyclic deformation). Since, according to eq. 2, the onset of residual stress relaxation depends on the resistance of the material R_i as well as on the applied stress σ , all the parameters characterizing the state of the material as well as temperature and time or frequency make themselves felt. The onset of residual stress-relaxation is delayed by the presence of sufficient stable obstacles to dislocation movement which increases R_i at the loads given. For $T < 0.4 T_m$ ($T_m =$ melting temperature in K) these could, for example, be grain and phase boundaries, finely dispersed incoherent particles, coarse secondary phases and, as long as no diffusion can occur, dissolved impurity atoms and certain dislocation arrangements. The onset and extent of residual stress-relaxation is influenced in a complex manner by the combined effects of heat treatment, unidirectional and cyclic stress and by multiaxial applied and/or residual stress states. The kinetics of residual stress-relaxation are determined essentially by the difference $\sigma + \sigma^{rs} - R_i$. The rate increases the greater the applied load, i. e. the higher the temperature, the longer the time and the

greater the magnitude and amplitude of the applied stress, plastic deformation or number of cycles. It often increases as the amount of residual stress increases. The rate is the faster the fewer the stable obstacles to dislocation glide are (4, 48).

7. Summary

The evaluation of the loading behaviour of shot peened components is only possible if sufficient knowledge of the shot peened state exists. It is important to know the formation processes of this state and all the peening parameters having an influence on it. The presented review shows that several methods and properties are necessary to give a precise description of shot peened surfaces. In most cases, it is sufficient to determine the depth distributions of residual stresses, the half-width values as a measure of the workhardening state, the surface roughness, and, if necessary, the phase fractions. In this connection, it is useful to discuss the texture pole figures as a special aspect. As a result of great experimental difficulties, only a few investigations in the microstructure with the aid of the transmission electron microscope exist. To extend the knowledge of the peening induced dislocation structures, such investigations are earnestly requested. Characteristic examples of the influence of the material conditions on the peening results are presented and discussed. During shot peening, mainly compressive residual stresses will be produced in the surface region of a material. In soft materials, these stresses result from surface workhardening and in hard materials (hardened steels, cold formed materials) from surface worksoftening.

8. References

- (1) Proc. First Int. Conf. on Shot Peening, Paris, 14. - 17.09.1981, Pergamon Press, Oxford (1982).
- (2) Proc. Second Int. Conf. on Shot Peening, Chicago. 14. - 17.05.1984, The American Shot Peening Society, Paramus, N.J. (1984).
- (3) B. Deffner: Dr.-Ing. thesis, Universität Karlsruhe (1982).
- (4) O. Vöhringer: In "Residual Stresses" (Ed. E. Macherauch, V. Hauk), DGM Informationsgesellschaft, Oberursel (1986) 47.
- (5) R. Kopp, K.-P. Hornauer: In (1) 541.
- (6) H. Wohlfahrt: In "Residual Stresses and Stress Relaxation", Sagamore Army Materials Res. Conf. Proc. (Ed. E. Kula, V. Weiss), Plenum Press, New York, Vol 28 (1982) 71.
- (7) H. Wohlfahrt: In (2) 316.
- (8) B. Scholtes, E. Macherauch: Z. Metallkde 77 (1986) 322.
- (9) K.-P. Hornauer: Dr.-Ing. thesis, RWTH Aachen (1982).
- (10) S. T. S. Al-Hassani: In (1) 583.
- (11) Y. Yokouchi, T. W. Chou, I. G. Greenfield: Metallurg. Trans. 14A (1983) 2415.
- (12) S. T. S. Al-Hassani: In (2) 275.
- (13) H. Guechichi, L. Castex, J. Frelat, G. Inglebert: In "Impact Surface Treatment (Ed. S. A. Meguid), Elsevier Appl. Sci. Publ. (1986) 11.
- (14) T. Hirsch, O. Vöhringer, E. Macherauch: Härterei-Techn. Mitt. 38 (1983) 229.

- (15) B. Scholtes: Unpublished results, Institut für Werkstoffkunde I, Universität Karlsruhe.
- (16) K.-P. Hornauer, H.-H. Jühe, A. Klinkenberg, P. Starker: Härterei-Techn. Mitt. 36 (1981) 322.
- (17) W. P. Evans, R. E. Ricklefs, J. F. Millan: Metallurgical Society Conferences, Vol. 36 (Ed. J. B. Cohen, J. E. Hilliard), Gordon and Breach Sci. Publ. (1965) 351.
- (18) H. Faber, O. Vöhringer, E. Macherauch: Härterei-Techn. Mitt. 34 (1979) 1.
- (19) G. K. Williamson, R. E. Smallman: Phil. Mag. 1 (1956) 34
- (20) J. Hoffmann: Dr.-Ing. thesis, Universität Karlsruhe (1985).
- (21) J. Hoffmann, H. Neff, B. Scholtes, E. Macherauch: Härterei-Techn. Mitt. 38 (1983) 180.
- (22) G. Maurer, H. Neff, B. Scholtes, E. Macherauch: Z. Metallkde. 78 (1987) 1.
- (23) D. Hakimi, C. Servant. L Castex: In (2) 249.
- (24) S. Pakrasi, J. Betzold: In (1) 193.
- (25) D. Kirk: In (1) 270.
- (26) P. Starker, E. Macherauch: Z. Werkstofftechnik 14 (1983) 109.
- (27) H. Harig, K. Middeldorf, K. Müller: Härterei-Techn. Mitt. 41 (1986) 286.
- (28) T. Hirsch, O. Vöhringer, E. Macherauch: In (2) 90.
- (29) O. Vöhringer, T. Hirsch, E. Macherauch: In "Proc. 5th Int. Conf. Titanium, München 1984 (Ed. G. Lütjering, U. Zwicker, W. Bunk), DGM Informationsgesellschaft, Oberursel, Vol. 4 (1985), 2203.
- (30) H. Wohlfahrt: In "Residual Stresses" (Ed. E. Macherauch, V. Hauk), DGM Informationsgesellschaft, Oberursel (1986) 347.
- (31) P. Strigens: Dr.-Ing. thesis, TH Darmstadt (1971).
- (32) L. Wagner: Dr.-Ing. thesis, Ruhr-Universität Bochum (1981).
- (33) A. Ebenau, O. Vöhringer, E. Macherauch: In Proc. I.C.S.P. 3.
- (34) P. Martin: Dr.-Ing. thesis, Hochschule der Bundeswehr, Hamburg (1980).
- (35) P. Starker: Dr.-Ing. thesis, Universität Karlsruhe (1981).
- (36) J. E. Hoffmann: Dr.-Ing. thesis, Universität Karlsruhe (1984).
- (37) R. Schreiber: Dr.-Ing. thesis, Universität Karlsruhe (1976).
- (38) R. Schreiber, H. Wohlfahrt, E. Macherauch: Archiv Eisenhüttenwesen 48 (1977) 649 und 653; 49 (1978) 37 und 265.
- (39) E. Macherauch, O. Vöhringer: Härterei-Techn. Mitt 41 (1986) 71.
- (40) J. L. Alshevskiy, G. V. Kurdjumov: Fiz. metal. metalloved. 30 (1970) 413.
- (41) K. Iida: In (2) 283.
- (42) A. Ebenau: unpublished results, Institut für Werkstoffkunde I, Universität Karlsruhe.
- (43) I. C. Noyan, J. B. Cohen: Mater. Sci. Eng. 75 (1985) 179.
- (44) C. Kim: Advances X-Ray Analysis 25 (1981) 343.
- (45) I. Schmidt: Journ Mater. Sci. Letters 5 (1986) 475.
- (46) K. H. Kloos, M. Koch, B. Kaiser: Z. Werkstofftechnik 17 (1986) 350.
- (47) M. James: In "Advances in Surface Treatments", Vol. 4 (Ed. A. Niku-Lari), Pergamon Press (1987) 349.
- (48) O. Vöhringer: In "Advances in Surface Treatments", Vol. 4 (Ed. A. Niku-Lari), Pergamon Press (1987) 367.